Title: Whole transcriptome-sequencing and network analysis of CD1c+ human dendritic cells identifies cytokine-secreting subsets linked to type I IFN-negative autoimmunity to the eye

Authors:

S. Hiddingh[1,3†], A. Pandit[3,4†], F.H. Verhagen[1-3†], R. Rijken[3,4], N. H. Servaas[3,4], C.G.K. Wichers[3,4], N.H. ten Dam-van Loon[2], S.M. Imhof[1,2], T.R.D.J. Radstake[5‡], J.H. de Boer[1,2‡], J.J.W. Kuiper[1-3‡*]

Affiliations:

[1] Ophthalmo-Immunology, University Medical Center Utrecht, Utrecht University, Utrecht, the Netherlands.

[2] Department of Ophthalmology, University Medical Center Utrecht, Utrecht University, Utrecht, the Netherlands.

[3] Center for Translational Immunology, University Medical Center Utrecht, Utrecht University, Utrecht, the Netherlands.

[4] Department of Rheumatology & Clinical Immunology, University Medical Center Utrecht, Utrecht University, Utrecht, the Netherlands.

[5] University Medical Center Utrecht and Utrecht University, Utrecht, The Netherlands and AbbVie, Chicago, IL.

[*] these authors contributed equally,

[†] these authors contributed equally.

* Corresponding author:

J.J.W. Kuiper J.J.W.Kuiper@umcutrecht.nl Heidelberglaan 100, 3584CX, Utrecht, The Netherlands.

Graphical Abstract:

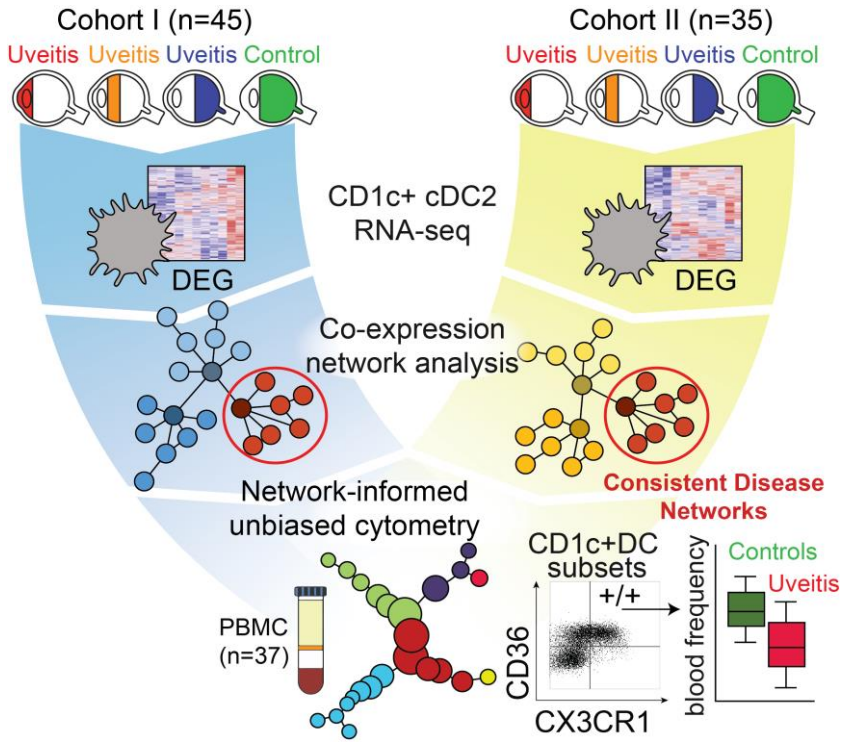

ABSTRACT

Background: Inflammatory subsets of CD1c+ conventional dendritic cells (CD1c+ DCs) are promoted by type I interferons (IFN), but the molecular basis for CD1c+ DCs involvement in conditions not driven by type I IFNs is unknown.

Methods: Our objective was to use RNA-sequencing of blood CD1c+ DCs and high-dimensional flow cytometry of two cohorts of autoimmune uveitis patients and healthy donors to characterize the CD1c+ DCs population of type I IFN-*negative* autoimmune uveitis.

Results: We report that the CD1c+ DCs pool from patients with autoimmune uveitis (n=45) is skewed towards a transcriptional network characterized by surface receptor genes *CX3CR1, CCR2,* and *CD36*. We confirmed the association of the transcriptional network with autoimmune uveitis by RNA-sequencing in another case-control cohort (n=35) and demonstrated that this network was governed by NOTCH2-RUNX3 signaling. Unbiased flow cytometry analysis based on the transcriptional network identified blood CD1c+ DC subsets that can be distinguished by CX3CR1 and CD36 surface expression. A CD36+CX3CR1+CD1c+ DC subset within the novel DC3 population was diminished in peripheral blood of patients, while CD1c+ DCs expressing *CD36* and *CX3CR1* accumulate locally in the inflamed eye. The CD36+CX3CR1+CD1c+ DC subset showed a differential capacity to produce cytokines, including TNF-alpha, IL-6, and VEGF, but not IL-23.

Conclusion: These results show that CD1c+ DC subsets defined on the basis of surface expression of CD36 and CX3CR1 are linked to type I IFN-negative human autoimmune uveitis and show a differential capacity to secrete proinflammatory mediators that drive its pathophysiology.

Main Text:

INTRODUCTION:

Autoimmune uveitis - or *non-infectious* uveitis- refers to a family of severe inflammatory eye conditions that are a leading cause of preventable vision loss in the Western world (*1,2*). The disease mechanisms of human autoimmune uveitis are poorly understood. T cells are considered to play a role in autoimmune uveitis predominantly based on a large body of mechanistic studies using *experimental autoimmune uveitis* (EAU) in rodents (*3,4*). In human autoimmune uveitis, it is unknown where and through which signals these T cells are activated. Genetic studies of archetypal forms of autoimmune uveitis; HLA-B27-associated anterior uveitis, idiopathic intermediate uveitis, and HLA-A29-associated Birdshot Uveitis, demonstrated strong genetic association with *HLA* and *ERAP* genes, indicating that antigen presentation is central to the etiology of autoimmune uveitis (*5-8*). Although the role of antigen presenting cells in autoimmune uveitis is under explored, dendritic cells – key antigen presenting cells - strongly promote EAU (*9-11*). Previous studies have shown that in blood, the proportion of CD1c+ conventional dendritic cells (CD1c+ DCs) is associated with disease activity (*12-14*), and dendritic cells increase in abundance in eye fluid of patients (*15*). Thus, it is important to understand the role of dendritic cells in autoimmune uveitis.

Recent single-cell studies have revealed that the human CD1c+ DC pool (and the murine equivalent termed “cDC2s”) constitute at least two phenotypically distinct subsets that originate from distinct progenitors (*16-18*). Cytokines of the type I Interferon (IFN) family have been shown to promote the expansion of a discrete subset within the CD1c+ DC pool in peripheral blood, termed “DC3” (*16,19,20*), which increase in frequency in blood during the type I IFN-driven condition *systemic lupus erythematosus* (SLE)(*17*). However, in contrast to SLE, uveitis disease activity in humans is accompanied by decreased type I IFN levels (21). More importantly, while the administration of type I Interferons can induce *lupus-like* disease, type I interferon therapy suppresses autoimmune uveitis (*21-23*), suggesting a distinct disease mechanism for CD1c+ DC involvement in human autoimmune uveitis. Therefore, our

understanding of the CD1c+ DC characteristics during autoimmunity is incomplete, especially for conditions not driven by type I IFNs.

Our objective was to use whole transcriptome profiling by bulk RNA-sequencing of peripheral blood CD1c+ DCs and multiparameter flow cytometry of two cohorts of autoimmune uveitis patients and healthy donors to characterize the core transcriptional features and subset composition of CD1c+ DCs in autoimmunity of the eye. We constructed data-driven co-expression networks that identified a core transcriptional circuit in patients that helped identify novel CD1c+ DC subsets that are functionally distinct and associated with autoimmune uveitis.

Results

An CD1c+ DC transcriptome cluster is associated with autoimmune uveitis

We aimed to characterize the transcriptome of CD1c+ DCs from patients with autoimmune uveitis (**Fig. 1A**). We purified CD1c+ DC cells from blood of 29 adult patients with anatomically distinct types of autoimmune uveitis (**Table 1**) and 16 age- and sex-matched controls and studied the transcriptome of the cell fractions by bulk RNA-sequencing (RNA-seq). We identified 6,794 differentially expressed genes (DEGs) at $P<0.05$ (power ≥ 0.8, see *methods*) between all groups (**Supplemental Table 6**). The expression profile of the DEGs split the samples into clear patient and control groups in the two-dimensional PCA subspace (**Fig. 1B**). To detect a biologically relevant higher order organization of the transcriptome, we constructed co-expression networks of the DEGs, which discerned 24 gene modules (**Fig. 1C**). Inspection of the module's *eigengene* values across the samples revealed that the 'black' module (1,236 DEGs) was the largest and associated with uveitis, regardless of disease subtype (**Fig. 1D**). Within the black module, transcripts encoding the chemokine receptors *CX3CR1* (Module Membership [MM] = 0.95, $P = 5.9 \times 10^{-22}$) and *CCR2* (MM = 0.92, $P = 1.8 \times 10^{-17}$) showed the highest module membership and thus best represent the expression pattern of the uveitis-associated module. The black module also includes *ESAM* and *CLEC12A* which encode for surface markers that distinguish mouse cDC2 subsets

(*24,25*). Because the surface receptors *CX3CR1* and *CCR2* have also been associated with distinct subsets cDC2s (*24,26,27*), we focused on the 100 genes in the black module that encode cell surface proteins (according to *surfaceome* predictor *SURFY*)(*28*) and their transcriptional regulation (**Supplemental Table 6**); In addition to *CX3CR1* and *CCR2*, the scavenger receptor *CD36*, and Toll like receptor (TLR) family members *1,4,6-8*, and *CD180*, all showed higher gene expression levels in CD1c+ DC cells of patients (**Fig. 1E**). Other surface receptor genes in this module were down-regulated in patients, including *SLC2A1* and *SLC7A5* (encoding the glucose and amino acid transporters GLUT1 and LAT1, respectively). Eight transcription factors previously shown to be linked to distinct human CD1c+ DC subsets (*29*) were also detected in the black module, including *RUNX3, IRF8,* and *NFKB1* (**Fig. 1E**).

The gene signature encompassing *CX3CR1*, *CCR2*, and *CD36* has been linked to a population within the CD1c+ DC pool with a 'monocyte-like' transcriptome (*16,24,30*). Although we observed CD14 expression in our CD1c+ fractions, there was no enrichment of CD14-positive cells in our patient samples used for RNA-seq (**Fig. 1F**) nor was *CD14* differentially expressed by RNA-seq (P_{LRT}= 0.32). To assess if the uveitis gene module was dependent on CD14 surface expression by CD1c+ DCs, we purified CD14-negative CD1c+ DCs from an independent cohort of 35 patients and controls and used bulk RNA-seq to study their transcriptome. Similar to the first cohort, the detected DEGs (n=2,016; P<0.05) clearly distinguished patients from controls by PCA (**Fig. 2A** and **Supplemental Table 7**). Co-expression network analysis of the DEGs from the second cohort identified six gene modules, of which three modules exhibited a significant number of overlapping co-expressed genes with the black module from the discovery cohort (**Fig. 2B**). In total, 147 DEGs of the black module in the first cohort were also co-expressed DEGs in the second cohort of patients and controls (**Fig. 2C**), of which 94% of these co-expressed genes also showed consistent direction of effect (e.g., upregulated in both cohorts)(**Fig. 2D**, **Supplementary Table 8**), which substantiates this gene set as a core transcriptional feature of human

autoimmune uveitis. Among the 147 genes we replicated *CX3CR1*, *CD36*, *CCR2*, *CCR5*, *CD36*, *TLR-6,-7,-8*, *CD180* (**Fig. 2E**), but also *TNFRSF1A* (the main TNF-alpha receptor), *CYBB,* (critically involved in T cell activation by DCs in autoimmune models) (*31*), and transcription factors *RUNX3*, *IRF8*, and *NFKBI* associated with cDC2 subsets (*18,29*). Note, *CCR2* and *CX3CR1* also showed high module membership in the second cohort (**Supplementary Table 8**). Collectively, these data show a core transcriptional signature in blood CD1c+ DCs of autoimmune uveitis patients.

Compromised NOTCH2-RUNX3 signaling recapitulates the transcriptional signature of autoimmune uveitis

To better understand the transcriptional regulation of the identified gene module, we generated module-specific regulator-target networks for each cohort using *RegEnrich* (*32*). After filtering for differentially and co-expressed expressed regulators (i.e., regulatory genes among the 147 genes with consistent direction of effect in both cohorts), we identified *RUNX3*, *IRF8*, *ATF4, JDP2, MEF2D*, *PATZ1,* and *NFKB1* as transcriptional regulators for the black module. Note that *RUNX3, IRF8,* and *NFKB1* also clustered into a single transcriptomic cluster in single cell analysis of human CD1c+ DC subsets by Brown and associates (*29*). Because loss of RUNX3 in mononuclear phagocytes (i.e. cDC2s) has been linked with chronic inflammation in mice models (*33*), we hypothesized that the signaling that involves the transcription factor *RUNX3* may promote the transcriptomic signature that characterize CD1c+ DCs of patients.

Efforts to study the effects of siRNA-mediated knockdown or CRISPR-Cas9-mediated knockout (KO) of *RUNX3* in CD1c+ DCs were unsuccessful (no knock-down or knock-out of *RUNX3* achieved). Therefore, we analyzed gene expression data of the (CD11b+) cDC2s (murine equivalent of human CD1c+ DCs) cells from CD11c-DC-*Runx3*Δ mice (*34*). Loss of *runx3* in murine cDC2s resulted in a gene expression profile that considerably recapitulates the gene module associated with autoimmune uveitis (**Fig. 3A**). In detail, we detected enrichment for many genes that are upregulated in *runx3*-KO cDCs2, including increased

expression levels for *cd36*, *ccr2*, and *cx3cr1* by gene-set enrichment analysis (GSEA) (**Fig. 3B**). This supports our hypothesis that the 'monocyte-like' signature genes (i.e. *CD36*, *CX3CR1*, *CCR2*) are regulated by RUNX3. Indeed, RUNX3 directly binds the promoter of *CD36* and negatively regulates its expression in myeloid cells (*35*). Importantly, overnight stimulation of MACS-sorted CD1c+ DCs by various key myeloid cytokines or Toll-like receptor (TLR) ligands did not result in a decrease in expression of *RUNX3* nor in a concordant increase in *CD36* expression, suggesting that the observed gene signature in the CD1c+ DC pool is unlikely to reflect an activation continuum (**Fig. 3C**). In fact, TLR-stimulation (with LPS, LTA, or R848) resulted in a strong upregulation of *RUNX3* and downregulation of CD36, which is the opposite of the expression pattern detected in patients. Also, overnight stimulation with cytokines GM-CSF and IFN-alpha that are implicated in the promotion of specific cDC2 subsets (*19,20*) did not decrease the expression of *RUNX3* (**Fig. 3C**). In general, the transcriptional signature of autoimmune uveitis did not resemble the gene signature of *in vivo* activated cDC2s (termed 'inflammatory' cDC2s' [*infcDC2s*]) (*36*). However, we did observe a significant positive enrichment score (NES=1.30, *Padj* = 0.02) for genes down-regulated in infcDC2s in the transcriptome of IU patients (**Fig. 3A** and **3B**).

Because murine studies underscored a Notch-dependent divergence of cDC2 subsets (*24*,*37*), we reasoned that the CD1c+ DC transcriptional signature driven by *RUNX3* of patients would be dependent on NOTCH2 signaling. To explore this, we investigated the transcriptome of dendritic cells of notch2Δ-CD11c mice (*38*). In agreement with the expression data of the CD11c-DC-Runx3Δ mice, loss of Notch2 resulted in up regulation of *ccr2*, *cd36*, *cx3cr1*, and decreased expression of *runx3* (**Fig. 3A**), and we detected enrichment for genes upregulated in *notch2*-KO cDCs2 (**Fig. 3B**). This supports that NOTCH2 is upstream of RUNX3 and mediates the transcriptomic characteristics of blood CD1c+ DCs of autoimmune uveitis. These findings were further strengthened in reanalysis of previously published transcriptomic data of murine bone marrow progenitors cultured for 7 days with OP9 stromal cells that express the NOTCH2 ligand DLL1 or OP-9 cells without

DLL1 (*39*). This analysis revealed that *notch2*-controlled genes were enriched in the transcriptome of CD1c+ DCs of patients and that notch2-signalling governs the expression of *cd36, ccr2, and cx3cr1* in cDC2s (**Fig. 3D** and **Fig. 3E).** To investigate if NOTCH2 was also important at more mature stages of cDC2 development (i.e., in dendritic cells that circulate in blood), we also generated CD1c+ DCs from human CD34+ hematopoietic progenitors in cultures with OP9-DLL1 (NOTCH2-stimulation), in which we inhibited NOTCH2 after CD1c+ DCs normally occur in culture at day 7. We used an anti-NOTCH2 antibody or an inhibitor for ADAM10, a key regulator of the NOTCH2 pathway involved in cDC2 biology (*40*) and measured the CD1c+ DC numbers at day 14. This analysis showed that late inhibition of NOTCH2 signaling substantially impaired the cell numbers of CD1c+ DCs in culture and supports that NOTCH2 signaling is actively involved in the maintenance of human CD1c+ DCs (**Supplemental Fig. S1**). Collectively, these observations support that compromised *NOTCH2-RUNX3* signaling promotes a transcriptomic signature that closely resembles the gene profile of CD1c+ DCs in human autoimmune uveitis.

A CD36+CX3CR1+CD1c+ DC3 subset is decreased in autoimmune uveitis

We reasoned that the transcriptomic signature of the CD1c+ DC pool in patients may be an impression of changes in the proportions of CD1c+ DC subsets in blood. To allow identification of undefined phenotypes, we first used unbiased flow cytometry data analysis to identify CD1c+ DC clusters in peripheral blood mononuclear cells (PBMCs) samples from 26 cases and 11 controls. We designed a panel based on genes from the uveitis gene signature (CD36, CX3CR1, CCR2, and CD180), surface markers previously linked to CD1c+ DC subsets, but that were not DEGs (CD5, and CD163) (*17*), and classical CD1c+ DC markers (CD1c and CD11c), and a lineage marker (CD3/CD19/CD56). FlowSOM (*41*) was used on singlets (PBMCs) to cluster cells into a predetermined number of 100 clusters (flowSOM default of 10 x 10 grid) to facilitate unbiased detection of possible CD1c+ DC phenotypes in blood. The analysis with flowSOM clearly distinguished four (Lin-HLA-DR+CD11c+) CD1c+ DC clusters (cluster number 41, 61, 81, and 83) (**Fig. 4A** and **Supplemental Fig. 2**). We

extracted the data for the four CD1c+ DC clusters (i.e., clusters 41, 61, 81, and 83) and conducted principal component analysis (PCA). The first two principal components explained 98.5% of the variance and the PCA biplot identified CX3CR1 and CD36 as top loadings, indicating that these proteins distinguish CD1c+ DC phenotypes in blood (**Fig. 4B**). We also repeated this analysis using Lineage-(CD3/CD56/CD19) HLA-DR+ cells as input for flowSOM clustering, which corroborated CD36 and CX3CR1 as key markers that distinguish CD1c+ DC phenotypes (**Supplemental Fig. 3**).

Next, we designed a simple gating strategy for CD1c+ DC subsets based on the expression of CD36 and CX3CR1 (**Fig. 4C**). Manual gating distinguished four CD1c+ DCs subsets; a CD36-CX3CR1- subset, a CD36+CX3CR1- subset and a rare CD36-CX3CR1+ subset, and a CD36+CX3CR1+ subset of CD1c+ DCs in peripheral blood. The CD36+CX3CR1- and CD36+CX3CR1+ subsets express both CD163 (**Fig. 4C**) and CD14 (**Fig. 4D** and **Supplementary Fig. 4**). Comparison between patients and controls revealed that the frequency of CD36+CX3CR1+ CD1c+ DCs were decreased in the blood of autoimmune uveitis patients (**Fig. 4E** and **4F**).

We speculated that the decrease in blood CD36+CX3CR1+ CD1c+ DCs was a result from migration of these cells to the eye during autoimmune uveitis. Recent single-cell RNA sequencing data by Kasper and co-workers in eye biopsies of autoimmune uveitis patients show infiltration in the eye by conventional dendritic cells, which are transcriptionally similar to CD1c+ DCs (*42*). Reanalysis of this data using *CLEC10A* as a specific marker for CD1c+ DCs in tissues (*43*) showed that eye-infiltrating CD1c+ DC cells express *CD36* and *CX3CR1* (**Fig. 4G**). Together, these results demonstrate that a specific CD36+CX3CR1+ subset of CD1c+ DCs was diminished in the blood of patients with autoimmune uveitis.

CD36 and CX3CR1 define functionally distinct CD1c+ DC subsets

Finally, we were interested if the identified CD36+CX3CR1+CD1c+ DC subset was functionally different from other CD1c+ DC subsets. To this end, we freshly sorted primary human CD1c+ DC subsets based on the surface expression of CD36 and CX3CR1 (**Fig.**

5A), of which double-positive and double-negative subsets could be sorted from the selected healthy subjects in sufficient numbers for experimental analysis. Since CD36 is a co-receptor for TLR2 (*44*), we overnight stimulated the subsets with the TLR2 ligand lipoteichoic acid (LTA). Interleukin (IL)-23, a cytokine potently produced by CD1c+ DCs in general, was equally strong secreted by both subsets of CD1c+ DCs (**Fig. 5B**). To assess the secretome of the CD1c+ DC subsets in more detail, we profiled the supernatants of LTA-stimulated CD1c+ DC subsets for additional soluble immune mediators: The CD1c+ DC subsets could be distinguished based on the secreted protein profile (**Fig. 5C**), of which the levels of TNF-alpha, IL-6, VEGF-A, and TNFR1 showed significant differences between the subsets (**Fig. 5D**). These results show that CD1c+ DC subsets defined on the basis of surface expression of CD36 and CX3CR1 show a differential capacity to secrete pro-inflammatory mediators that participate in the pathophysiology of human autoimmune uveitis.

Discussion

In this study of 80 autoimmune uveitis patients and controls, we identified and replicated a core disease transcriptional network in CD1c+ DCs. We were able to track back the network to a cytokine-producing CD36+CX3CR1+ CD1c+ DC subset that was diminished in peripheral blood of patients with autoimmune uveitis.

Using data from genetic models, we show that reciprocal expression of the gene network associated with autoimmune uveitis relies on transcription factors NOTCH2 and RUNX3. Brown *et al*., (*29*) recently showed that in human blood CD1c+ DCs the differential expression of transcription factors, including *RUNX3*, *IRF8*, and *NFKB1* (which were all in the transcriptional signature of CD1c+ DCs of patients) delineate CD1c+ DC subsets. Our observation that these transcription factors were differentially co-expressed support that the gene expression changes identified in uveitis patients were mediated by compositional changes in discrete subsets with reciprocal gene expression patterns (*16*).

Other preceding studies into human CD1c+ DCs revealed functionally distinct subsets termed “DC2” and “DC3”, with the DC3 showing both transcriptomic features reminiscent of

cDC2s and monocytes - such as elevated *CD36* levels (*16*). DC3s also have distinct developmental pathways and transcriptional regulators compared to DC2 (*16-18,20*). Recently, Cytlak and associates revealed that lower expression of *IRF8* is linked to DC3 (*20*), a transcription factor that was also decreased in autoimmune uveitis. Dutertre and co-workers (*17*) showed that the phenotype of peripheral blood CD1c+ DCs can be further segregated according to the expression of CD163 and CD5, with "DC3" cells being characterized as CD5-CD163+ cells and "DC2" as CD5+CD163 cells. We show that CD1c+ DCs can also be segregated based on surface expression of CD36 and CX3CR1 and that DC3s (CD1c+CD5-CD163+) are found both in the CD36+CX3CR1- and CD36+CX3CR1+ subsets. In other words, CD36 and CX3CR1 surface expression defines phenotypically discrete DC3 subsets in peripheral blood. The CD36-CX3CR1- subset was CD5+CD163- and similar to DC2 cells (*12*). Patients with *Systemic lupus erythematosus* (SLE) display accumulation of CD5-CD163+ DC3s in blood (*13*), while this population of DC3 cells (CD5-CD163+CD1c+ DCs) was decreased in autoimmune uveitis patients (**Fig. 4)**. The differences between autoimmune uveitis and SLE may be related to distinct (i.e., opposite) immunopathological mechanisms; Type I interferons drive the maturation of cDC2s into "inflammatory cDC2s" (infcDC2s)(*36*) and can induce CD1c+ DCs to express a distinct set of surface-receptors (*19*). The type I interferon (IFN)-α drives immunopathology of SLE (*21*) and administration of type I interferon therapy can induce *lupus-like* disease (*22,23*). In favor of attributing the seemingly contrasting observations in blood CD1c+ subsets between SLE and autoimmune uveitis to distinct biology is the fact that, in contrast to elevated IFN-α in patients with SLE, in autoimmune uveitis patient's disease exacerbations correlate with reduced blood IFN-α concentrations (*21*). In addition, we demonstrated that the transcriptional signature of CD1c+ DCs in autoimmune uveitis was not positively enriched for transcriptomic features of IFN-driven cDC2 subset (**Fig. 3B**).

This also indicates that unlike SLE (*45*), changes of the CD1c+ DC peripheral blood pool in autoimmune uveitis are not driven by increased type I interferon signaling (*21*), but rather by

yet unspecified pathological molecular pathways. This is supported by the fact that in our stimulation experiments, IFN alpha did not induce the uveitis gene signature in CD1c+ DCs (**Fig. 3**) and that type I interferon therapy inhibits autoimmune uveitis (*21*). However, an argument against this is the observation that in IU patients we detected enrichment for genes down-regulated in infcDC2s (*20,36*). Indeed, although not all statistically significant, genes such as *ccr2*, *cd36*, *cx3r1* show a relative decrease in expression, while *runx3* shows a relative increase in expression in the transcriptome of *infcDC2s* versus "non-inflammatory" cDC2s (based on GSE149619). In other words, this suggest that the profile of *infcDC2s* within the CD1c+DC pool was 'decreased' in IU patients, which is in line with the decrease in the frequency of CD5-CD163 DC3s as a whole or the TNF-alpha and IL-6-secreting CD36+CX3CR1+ DC3 subset in patients with autoimmune uveitis. One possible explanation for the decrease in this subset may be that in the systemic condition SLE 'inflammatory' DC3s 'accumulate' in blood, while in autoimmune uveitis this population exits the circulation to infiltrate secondary lymphoid tissues and ocular structures to mediate eye inflammation. Indeed, emerging single cell analysis of ocular fluids of patients support the infiltration of CD1c+ DC subsets in the eye during autoimmune uveitis (*42*), and we show that these cells express *CD36* and *CX3CR1* (**Fig. 4G**). However, ideally longitudinal data are used to follow the dynamics of these populations in patients in relation to disease activity, which is a limitation of the current study.

Other disease modifying factors possibly affect the CD1c+ DC pool in uveitis patients. In mice, antibiotic treatment to experimentally disturb the microbiota affects a cDC2 subset phenotypically similar to CD1c+ DCs and decreases their frequency in the intestine of mice, which suggests microbiota-dependent signals involved in the maintenance of cDC2 subsets (*16*). This is especially interesting in light of growing evidence that microbiota dependent signals cause autoreactive T cells to trigger uveitis (*46,47*), which makes it tempting to speculate that gut-resident cDC2 subsets contribute to the activation of T cells in uveitis models. Dietary components can influence subsets of intestinal dendritic cells (*48*).

Regardless, most likely, an ensemble of disease modulating factors is involved. For example, myeloid cytokines, such as GM-CSF, contribute to autoimmunity of the eye (*49*) and GM-CSF has been shown to stimulate the differentiation of human CD1c+ subset from progenitors (*20*). However, GM-CSF signaling in conventional dendritic cells has a minor role in the inception of EAU (*49,50*). Our data supports that stimulation of CD1c+ subsets with GM-CSF or TLR ligands does not induce the transcriptional features of CD1c+ DCs during autoimmune uveitis, which is in line with previous observations that support that stimulated cDC2s do not convert from one into another subset (*20*). Note that key transcription factors (e.g. *RUNX3*) defining the here identified CD1c+ subsets are definitely affected by TLR stimulation (**Fig. 3C**), but the overall transcriptomic program of activated CD1c+ DCs is distinct (**Fig. 3B**).

Better understanding of the changes in the CD1c+ DC pool during human autoimmune uveitis will help develop strategies to pharmacologically influence putative disease pathways involved at an early disease stage, which may lay the foundation for the design of effective strategies to halt progress towards severe visual complications or blindness. Perhaps targeting CD1c+ DCs may be achieved by dietary (microbiome) strategies and provide relatively safe preventive strategies for noninfectious uveitis.

In conclusion, we discovered a CD36+CX3CR1+CD1c+ DC subset that decreased in the peripheral blood of patients with autoimmune uveitis. The fact that this population secretes high levels of TNF-alpha, is decreased in the circulation of patients, while CD1c+ DCs expressing *CD36* and *CX3CR1* accumulate locally in autoimmune uveitis patients may not only explains the therapeutic benefit of TNF inhibition for autoimmune uveitis, it also opens new avenues for therapeutic targeting to prevent blindness due to autoimmune uveitis.

MATERIAL AND METHODS

Patients and patient material

This study was conducted in compliance with the Helsinki principles. Ethical approval was requested and obtained from the Medical Ethical Research Committee in Utrecht. All patients signed written informed consent before participation. We collected blood from a discovery cohort of 29 and a replication cohort of 22 adult patients (**Table 1**) with HLA-B27-associated Acute Anterior Uveitis (AU), Idiopathic Intermediate Uveitis (IU), or HLA-A29-associated Birdshot Uveitis (BU). Patients were recruited at the outbound patient clinic of the department of Ophthalmology of the University Medical Center Utrecht between July 2014 and January 2017. No minimize bias we recruited twenty-nine age and sex matched anonymous blood donors of European Ancestry with no history of ocular inflammatory disease at the same institute to served as unaffected controls (16 for the discovery cohort and 13 for the replication cohort). Uveitis was classified and graded in accordance with the SUN classification (*51*). Each patient underwent a full ophthalmological examination by an ophthalmologist experienced in uveitis, routine laboratory screening, and an X-Ray of the lungs. Laboratory screening included erythrocyte sedimentation rate, renal and liver function tests, angiotensin converting enzyme (ACE), and screening for infectious agents in the serum and an Interferon-Gamma Release Assay (IGRA) was obtained for all patients. All patients with AU and BU were HLA-B27 or HLA-A29-positive, respectively (confirmed by HLA typing). All patients had active uveitis (new onset or relapse) and there was no clinical evidence for uveitis-associated systemic inflammatory disease (e.g., rheumatic condition) till the time of sampling. None of the patients received systemic immunomodulatory treatment in the last 3 months, other than low dose (≤10mg) oral prednisolone in one BU patient of the discovery cohort and one AU patient of the replication cohort.

CD1c+ DC purification

Peripheral blood mononuclear cells (PBMCs) were isolated by standard ficoll density gradient centrifugation from 70mL heparinized blood immediately after blood withdrawal (GE Healthcare, Uppsala, Sweden). For the discovery cohort, fresh PBMCs were immediately subjected to magnetic-activated cell sorting (MACS) for the removal (positive selection) of

CD304+ cells (pDC), followed by CD19+ cells (B cell), and subsequently isolation of CD1c+ cells by using the CD1c+ (BDCA1) isolation kit (Miltenyi Biotec, Germany) according to the manufacturer's instructions. The isolated CD1c+ fraction contained on average 147,114 cells (range 46,000-773,000) and purity was determined by flow cytometry measured on the BD LSR Fortessa™ Cell analyzer (**Supplementary Table 1**). Data were analyzed using FlowJo software (TreeStar Inc.). For the replication cohort, ten batches (individual days) of 4-5 randomly selected patient and control samples of nitrogen stored PBMCs (mean storage time of 11 [range 0-31] months) were carefully thawed and subjected to sorting by the BD FACSAria™ III sorter after incubation with a panel of surface antibodies (**Supplementary Table 2**) and FACS buffer (1% bovine serum albumin and 0.1% sodium azide in phosphate buffered saline). CD3-CD19-CD56-HLA-DR+CD11c+CD1c+CD14- cells were sorted. The average number of collected cells by sorting was 56,881 (range 6,669-243,385). MACS or FACS purified CD1c+ cells were immediately taken up in a lysis buffer (RLT plus, Qiagen) containing 1% β-mercaptoethanol, snap frozen on dry ice, and stored at -80°C until RNA extraction was performed. Isolation of CD1c+ DC for functional experiments was done by MACS as described above. Purification of CD1c+ DC subsets (based on CD36 and CX3CR1 expression) from freshly isolated PBMCs was conducted by flow cytometry using the panel in **Supplementary Table 3**.

CD1c+ DC cultures

Purified CD1c+ DCs were cultured in RPMI Glutamax (Thermo Fisher Scientific) supplemented with 10% heat-inactivated fetal bovine serum (FBS) (Biowest Riverside) and 1% penicillin/streptomycin (Thermo Fisher Scientific). CD1c+ DCs were cultured at a concentration of 0.5×10^6 cells/mL in a 96-well round-bottom plate (100µL/well). Cells were stimulated overnight (18 hours) with multiple stimuli listed in **Supplementary Table 4**. After stimulation, supernatants were collected and frozen at -80°C until cytokine production analysis. Cells were lysed in an *RLT plus* lysis buffer (Qiagen) and stored at -80°C until RNA extraction was performed. In separate cultures, CD1c+ DC subsets (based on CD36 and

CX3CR1 expression) were cultured in the presence of 1µg/mL Lipoteichoic acid (LTA). After 18 hours of stimulation, supernatants were harvested and IL-23 cytokine production was analyzed by ELISA (R&D Systems). Cell lysates were stored at -80°C until RNA extraction was performed for qPCR. The levels of IL-2, IL-5, IL-6, IL-10, IL-12p70, IL-13, IL-17, IL-22, IL-27, TNF-alpha, IFN-alpha, IFN-beta, CCL1, CXCL10, CXCL13, VEGF, CD40L, FAS, TNFR1, TNFR2, Elastase, and Granzyme B were simultaneously measured in supernatant of CD1c+ DC cultures using the in-house multiplex immunoassay based on Luminex technology. Protein concentrations that were out of range were replaced with the LLOQ (lower limit of quantification) and ULOQ (upper limit of quantification) for each analyte and divided by 2 for the proteins detected below the range of detection or multiplied by 2 for values above the detection range.

Ex vivo generation of dendritic cells

CD1c+ Dendritic cells were generated from primary human CD34+ cells following the protocol of Kirkling and coworkers (*52*). Briefly, umbilical cord blood (CB) was collected after informed consent was obtained according to the Declaration of Helsinki. The ethics committee of the University Medical Center Utrecht approved these collection protocols (protocol number TC-bio 15-345). CB mononuclear cells were isolated from human umbilical CB by density centrifugation over Ficoll-Paque solution (GE Healthcare). CD34+ cells were isolated using anti-CD34 magnetic beads following the manufacturer's instructions (Miltenyi Biotec). CD34+ cells were cryopreserved until further use. OP-9 cells expressing DLL1 (NOTCH ligand) were cultured with MEM alpha Glutamax (Gibco) containing 20% heat-inactivated FBS (Biowest Riverside) and 1% penicillin/streptomycin (Thermo Fisher Scientific). CD34+ cells (10.000 cells/well) were plated onto 24-well plates coated with OP-9 cells (20.000 cells/well) and cultured in medium containing 20ng/mL SCF, 100ng/mL FLT3 ligand and 10ng/mL GM-CSF (all from Peprotech). After 7 days of culture, fresh media containing either 10µM ADAM10 inhibitor (GI 254023X; R&D systems), 50ng/mL anti-NOTCH2 (clone B6; Absolute Antibody) or a combination of the inhibitors were added to the

cells and cultured for another 7 days. Cells were harvested and used for FACS analysis on day 14.

Real-time Quantitative PCR

First-strand cDNA was synthesized from total RNA using Superscript IV kit (Thermo Fisher Scientific), and quantitative real-time PCR (RT-qPCR) was performed on the QuantStudio 12k flex System (LifeTechnologies), following manufacturer's instructions. Sequences of the primers used are listed in **Supplementary Table 5.** RT-qPCR data were normalized to the expression of the selected housekeeping gene *GUSB* (ENSG00000169919). CT values were normalized to *GUSB* by subtracting the CT mean of *GUSB* (measured in duplo) from the CT mean of the target mRNA (i.e., *CD36*, *RUNX3).* The resulting value is referred to as the ΔCT. The fold change (FC) of each sample was calculated in relation to the ΔCt of the medium control according to the formula FC = 2−ΔΔCt, where ΔΔCt = ΔCt sample—ΔCt reference.

Phenotyping CD1c+ DC populations in uveitis patients

PBMC samples from the discovery and replication cohort (HC 11 samples; AU 9 samples; IU 6 samples; BS 11 samples) were randomly selected and measured by flow cytometry in batches of 9 to 10 mixed samples per run, divided over 4 days. Per batch, 10 million PBMCs per sample were quickly thawed, washed with ice cold PBS and stained with the antibody panel depicted in **Supplementary Table 3**. PBMCs were incubated with Fixable Viability Dye eF780 (eBioscience) at room temperature for 10 minutes. Cells were then plated in V-bottomed plates (Greiner Bio- one), washed with PBS and incubated for 30 minutes at 4˚C in the dark with Brilliant Stain Buffer (BD) and the fluorescently- conjugated antibodies. Next, the cells were washed and taken up in the FACS buffer. Flow cytometric analyses were performed on the BD FACSAria™ III sorter. Manual gating of data was done using FlowJo software (TreeStar inc. San Carlos, CA, USA). FlowSOM (*41*) analysis was done as described previously (*53*). Single-cell data (FSC- A versus FSC- H gate) or Lin- (negative for CD3/CD56/CD19) HLA-DR+ data were transformed using the *logicleTransform* function of

the *flowCore R* package (*54*). The SOM was trained for a 10x10 grid (100 clusters) with 2000 iterations, or 7x7 grid (49 clusters) for Lin-HLA-DR+ cells. Consensus hierarchical clustering was used to annotate clusters, based on the ConsensusClusterPlus R package (*55*). Principal component analysis (PCA) analysis was done on normalized expression data from flowSOM using the *factoextra* R package.

RNA isolation and RNA sequencing

Total RNA from CD1c+ DC cell lysates from patients and controls was isolated using the AllPrep Universal Kit (Qiagen) on the QIAcube (Qiagen) according to the manufacturer's instructions. Library preparation and Illumina sequencing was performed on 44 samples of the discovery cohort at BGI (Hong Kong). RNA-seq libraries were generated with the TruSeq RNAseq RNA Library Prep Kit (Illumina Inc., Ipswich, MA, USA) and were sequenced using Illumina NextSeq 500 generating approximately 20 million 100bp paired end reads for each sample. For the replication cohort, RNA-seq libraries were generated by *GenomeScan* (Leiden, the Netherlands) with the TruSeq RNAseq RNA Library Prep Kit (Illumina Inc., Ipswich, MA, USA), and were sequenced using Illumina HiSeq 4000 generating ~20 million 150bp paired ended reads for each sample.

Power analysis

We conducted power analysis of the discovery cohort using the PROPER R package (version 1.22.0)(*56*) with 100 simulations of the *build-in* RNA-seq count data from antigen presenting (B) cells from a cohort of 41 individuals (i.e., large biological variation as expected in our study) (*57*). Simulations parameters used the default of 20,000 genes and an estimated 10% of genes being differentially expressed. We detected 0.8 power to detect differentially expressed genes ($P<0.05$) at a $\log_2$(fold change)>1 for the smallest patient group (9 cases) and we considered the sample size reasonable for analysis.

Differential gene expression and statistical analysis

Quality check of the raw sequences was performed using the FastQC tool. Reads were aligned to the human genome (GRCh38 build 79) using STAR aligner (*58*) and the Python package HTSeq was used to count the number of reads overlapping each annotated gene (*59*). We aligned the reads of the RNA sequencing data sets to 65,217 annotated *Ensemble Gene* IDs. Raw count data were fed into the DESeq2 (*60*) to identify differentially expressed genes (DEGs) between the four disease groups (AU, IU, BU, HC). Using DESeq2, we modelled the biological variability and overdispersion in expression data following a negative binomial distribution. We then used Wald's test to identify DEGs in each pair-wise comparison and used likelihood ratio test to identify DEGs considering multiple disease groups. We constructed co-expression gene networks ($\beta = 6$) with the WGCNA R package (61) using the cumulative differentially expressed genes ($P<0.05$) from all pairwise and group comparisons. We calculated the intersect between the modules constructed from the two cohorts and used Fisher's exact test to identify modules that exhibited significant overlap in genes. Pathway enrichment analysis was done with *ToppGene* Suite (BMI CCHMC, Cincinnati, OH, USA)(*62*).

Module specific regulator-target networks were generated using the *RegEnrich* R package (*32*). Gene expression data from *runx3*-knockout(KO) cDC2s, *notch2*-KO cDC2s, and inflammatory cDC2s were obtained from the NCBI Gene Expression Omnibus (accession numbers GSE48590 [2 wild-type [WT] CD11b+Esam+ splenic cDC2s versus 2 CD11b+Esam+ cDC2s from CD11c-DC-*Runx3*Δ mice], GSE119242 [2 untreated cDC2 versus untreated cDC2 from CD11c-Cre *notch2*f/f mice], GSE149619 [5 CD172+MAR1- cDC2s in mock condition vs 3 CD172+MAR1+ cDC2 in virus (flu) condition]) using GEO2R in the GEO database, which builds on the *GEOquery* and *limma* R packages (*63,64).* RNA-seq data from the mouse bone marrow stromal cell line OP9 expressing NOTCH ligand DLL1 (OP9-DLL1)-driven cDC2 cultures (GSE110577, [2 sorted CD11c+MHCII+B220−CD11b+ cDC2 from bone marrow cultures with FLT3L for 7 days vs 2 sorted CD11c+MHCII+B220−CD11b+ cDC2 from bone marrow cultures with FLT3L + OP9-DLL1 cells for 7 days]) were analyzed using *DESeq2* and normalized count data plotted using the

plotCounts function. Gene set enrichment analysis was done using the Fast Gene Set Enrichment Analysis R package and data plotted using the *GSEA.barplot* function from the *PPInfer* R package (*65*). Gene sets for *runx3*-KO, *notch2*-KO, inflammatory cDC2s, and cDC2s from OP9-DLL1 bone marrow cultures were generated by taking the top or bottom percentiles of ranked [$-\log_{10}(P) \times \text{sign}(\log_2(\text{fold change}))$] genes from each data set as indicated.

Data and Code Availability

The data code, bulk RNA-Seq datasets, flow cytometry dataset, and cytokine expression dataset in this publication will be made available via https://dataverse.nl/ doi:XXXX and deposited in NCBI's Gene Expression Omnibus accessible through GEO Series accession number GEO:XXXX.

Supplementary Materials

Fig. S1. Flow cytometry analysis of CD1c+ DC cells generated from CD34+ hematopoietic cord blood after NOTCH2 and ADAM10 inhibition.

Fig. S2. FlowSOM results for CD1c+ DC clusters in PBMCs.

Fig. S3. FlowSOM analysis using Lineage (CD3/CD19/CD56) negative and HLA-DR-positive cells as input.

Fig. S4. Flow cytometry gating example of CD1c+ CD11c+ DCs subsets based on CD36 and CX3CR1.

Table S1-Table S8

References

1. Thorne JE, Suhler E, Skup M, Tari S, Macaulay D, Chao J, Ganguli A. Prevalence of Noninfectious Uveitis in the United States: A Claims-Based Analysis. JAMA Ophthalmol. 2016 Nov 1;134(11):1237-1245.

573 2. Suttorp-Schulten MS, Rothova A. The possible impact of uveitis in blindness: a literature
574 survey. Br J Ophthalmol. 1996 Sep;80(9):844-8.
575 3. Lee RW, Nicholson LB, Sen HN, Chan CC, Wei L, Nussenblatt RB, Dick AD. Autoimmune and
576 autoinflammatory mechanisms in uveitis. Semin Immunopathol. 2014 Sep;36(5):581-94.
577 4. Caspi RR. A look at autoimmunity and inflammation in the eye. J Clin Invest. 2010
578 Sep;120(9):3073-83.
579 5. Kuiper JJW, Venema WJ. HLA-A29 and Birdshot Uveitis: Further Down the Rabbit Hole. Front
580 Immunol. 2020 Nov 11;11:599558.
581 6. Huang XF, Li Z, De Guzman E, Robinson P, Gensler L, Ward MM, Rahbar MH, Lee M, Weisman
582 MH, Macfarlane GJ, Jones GT, Klingberg E, Forsblad-d'Elia H, McCluskey P, Wakefield D,
583 Coombes JS, Fiatarone Singh MA, Mavros Y, Vlahovich N, Hughes DC, Marzo-Ortega H,
584 7. Kuiper JJW, Setten JV, Devall M, Cretu-Stancu M, Hiddingh S, Ophoff RA, Missotten TOAR,
585 Velthoven MV, Den Hollander AI, Hoyng CB, James E, Reeves E, Cordero-Coma M, Fonollosa
586 A, Adán A, Martín J, Koeleman BPC, Boer JH, Pulit SL, Márquez A, Radstake TRDJ.
587 8. Márquez A, Cordero-Coma M, Martín-Villa JM, Gorroño-Echebarría MB, Blanco R, Díaz Valle
588 D, Del Rio MJ, Blanco A, Olea JL, Cordero Y, Capella MJ, Díaz-Llopis M, Ortego-Centeno N,
589 Ruiz-Arruza I, Llorenç V, Adán A, Fonollosa A, Ten Berge J, Atan D, Dick AD,
590 9. Chen M, Liang D, Zuo A, Shao H, Kaplan HJ, Sun D. An A2B Adenosine Receptor Agonist
591 Promotes Th17 Autoimmune Responses in Experimental Autoimmune Uveitis (EAU) via
592 Dendritic Cell Activation. PLoS One. 2015 Jul 6;10(7):e0132348.
593 10. Fu Q, Man X, Wang X, Song N, Li Y, Xue J, Sun Y, Lin W. CD83+ CCR7+ NK cells induced by
594 interleukin 18 by dendritic cells promote experimental autoimmune uveitis. J Cell Mol Med.
595 2019 Mar;23(3):1827-1839.
596 11. Wang B, Tian Q, Guo D, Lin W, Xie X, Bi H. Activated γδ T Cells Promote Dendritic Cell
597 Maturation and Exacerbate the Development of Experimental Autoimmune Uveitis (EAU) in
598 Mice. Immunol Invest. 2021 Feb;50(2-3):164-183.
599 12. Chen P, Urzua CA, Knickelbein JE, Kim JS, Li Z, Hannes S, Kuo D, Chaigne-Delalande B,
600 Armbrust K, Tucker W, Liu B, Agrón E, Sen HN, Nussenblatt RB. Elevated CD1c+ Myeloid
601 Dendritic Cell Proportions Associate With Clinical Activity and Predict Disease Rea
602 13. Chen P, Denniston A, Hannes S, Tucker W, Wei L, Liu B, Xiao T, Hirani S, Li Z, Jawad S, Si H, Lee
603 RW, Sen HN, Nussenblatt RB. Increased CD1c+ mDC1 with mature phenotype regulated by
604 TNFα-p38 MAPK in autoimmune ocular inflammatory disease. Clin Immunol. 2
605 14. Chen P, Tucker W, Hannes S, Liu B, Si H, Gupta A, Lee RW, Sen HN, Nussenblatt RB. Levels of
606 blood CD1c+ mDC1 and CD1chi mDC1 subpopulation reflect disease activity in noninfectious
607 uveitis. Invest Ophthalmol Vis Sci. 2014 Dec 16;56(1):346-52.
608 15. O'Rourke M, Fearon U, Sweeney CM, Basdeo SA, Fletcher JM, Murphy CC, Canavan M. The
609 pathogenic role of dendritic cells in non-infectious anterior uveitis. Exp Eye Res. 2018
610 Aug;173:121-128.
611 16. Villani AC, Satija R, Reynolds G, Sarkizova S, Shekhar K, Fletcher J, Griesbeck M, Butler A,
612 Zheng S, Lazo S, Jardine L, Dixon D, Stephenson E, Nilsson E, Grundberg I, McDonald D, Filby
613 A, Li W, De Jager PL, Rozenblatt-Rosen O, Lane AA, Haniffa M, Regev
614 17. Dutertre CA, Becht E, Irac SE, Khalilnezhad A, Narang V, Khalilnezhad S, Ng PY, van den
615 Hoogen LL, Leong JY, Lee B, Chevrier M, Zhang XM, Yong PJA, Koh G, Lum J, Howland SW,
616 Mok E, Chen J, Larbi A, Tan HKK, Lim TKH, Karagianni P, Tzioufas AG, Malleret B,
617 18. Cytlak U, Resteu A, Pagan S, Green K, Milne P, Maisuria S, McDonald D, Hulme G, Filby A,
618 Carpenter B, Queen R, Hambleton S, Hague R, Lango Allen H, Thaventhiran JED, Doody G,
619 Collin M, Bigley V. Differential IRF8 Transcription Factor Requirement Defines
620 19. Girard M, Law JC, Edilova MI, Watts TH. Type I interferons drive the maturation of human
621 DC3s with a distinct costimulatory profile characterized by high GITRL. Sci Immunol. 2020
622 Nov 13;5(53):eabe0347.

20. Bourdely P, Anselmi G, Vaivode K, Ramos RN, Missolo-Koussou Y, Hidalgo S, Tosselo J, Nuñez N, Richer W, Vincent-Salomon A, Saxena A, Wood K, Lladser A, Piaggio E, Helft J, Guermonprez P. Transcriptional and Functional Analysis of CD1c+ Human Dendritic Ce
21. Wang W, Chong WP, Li C, Chen Z, Wu S, Zhou H, Wan Y, Chen W, Gery I, Liu Y, Caspi RR, Chen J. Type I Interferon Therapy Limits CNS Autoimmunity by Inhibiting CXCR3-Mediated Trafficking of Pathogenic Effector T Cells. Cell Rep. 2019 Jul 9;28(2):486-497.e4
22. Rönnblom LE, Alm GV, Oberg KE. Autoimmunity after alpha-interferon therapy for malignant carcinoid tumors. Ann Intern Med. 1991 Aug 1;115(3):178-83.
23. Rönnblom LE, Alm GV, Oberg KE. Possible induction of systemic lupus erythematosus by interferon-alpha treatment in a patient with a malignant carcinoid tumour. J Intern Med. 1990 Mar;227(3):207-10.
24. Lewis KL, Caton ML, Bogunovic M, Greter M, Grajkowska LT, Ng D, Klinakis A, Charo IF, Jung S, Gommerman JL, Ivanov II, Liu K, Merad M, Reizis B. Notch2 receptor signaling controls functional differentiation of dendritic cells in the spleen and intestine.
25. Kasahara S, Clark EA. Dendritic cell-associated lectin 2 (DCAL2) defines a distinct CD8α- dendritic cell subset. J Leukoc Biol. 2012 Mar;91(3):437-48.
26. Fujita K, Chakarov S, Kobayashi T, Sakamoto K, Voisin B, Duan K, Nakagawa T, Horiuchi K, Amagai M, Ginhoux F, Nagao K. Cell-autonomous FLT3L shedding via ADAM10 mediates conventional dendritic cell development in mouse spleen. Proc Natl Acad Sci U S A. 2
27. Nakano H, Lyons-Cohen MR, Whitehead GS, Nakano K, Cook DN. Distinct functions of CXCR4, CCR2, and CX3CR1 direct dendritic cell precursors from the bone marrow to the lung. J Leukoc Biol. 2017 May;101(5):1143-1153.
28. Bausch-Fluck D, Goldmann U, Müller S, van Oostrum M, Müller M, Schubert OT, Wollscheid B. The in silico human surfaceome. Proc Natl Acad Sci U S A. 2018 Nov 13;115(46):E10988-E10997.
29. Brown CC, Gudjonson H, Pritykin Y, Deep D, Lavallée VP, Mendoza A, Fromme R, Mazutis L, Ariyan C, Leslie C, Pe'er D, Rudensky AY. Transcriptional Basis of Mouse and Human Dendritic Cell Heterogeneity. Cell. 2019 Oct 31;179(4):846-863.e24.
30. Schrøder M, Melum GR, Landsverk OJ, Bujko A, Yaqub S, Gran E, Aamodt H, Bækkevold ES, Jahnsen FL, Richter L. CD1c-Expression by Monocytes - Implications for the Use of Commercial CD1c+ Dendritic Cell Isolation Kits. PLoS One. 2016 Jun 16;11(6):e0157387.
31. Keller CW, Kotur MB, Mundt S, Dokalis N, Ligeon LA, Shah AM, Prinz M, Becher B, Münz C, Lünemann JD. CYBB/NOX2 in conventional DCs controls T cell encephalitogenicity during neuroinflammation. Autophagy. 2020 May 13:1-15.
32. Tao W, Radstake RDJ, Pandit A. RegEnrich: An R package for gene regulator enrichment analysis reveals key role of ETS transcription factor family in interferon signaling. bioRxiv 2021.01.24.428029
33. Hantisteanu S, Dicken Y, Negreanu V, Goldenberg D, Brenner O, Leshkowitz D, Lotem J, Levanon D, Groner Y. Runx3 prevents spontaneous colitis by directing the differentiation of anti-inflammatory mononuclear phagocytes. PLoS One. 2020 May 26;15(5):e023304
34. Dicken J, Mildner A, Leshkowitz D, Touw IP, Hantisteanu S, Jung S, Groner Y. Transcriptional reprogramming of CD11b+Esam(hi) dendritic cell identity and function by loss of Runx3. PLoS One. 2013 Oct 15;8(10):e77490.
35. Puig-Kröger A, Domínguez-Soto A, Martínez-Muñoz L, Serrano-Gómez D, Lopez-Bravo M, Sierra-Filardi E, Fernández-Ruiz E, Ruiz-Velasco N, Ardavín C, Groner Y, Tandon N, Corbí AL, Vega MA. RUNX3 negatively regulates CD36 expression in myeloid cell lines. J I
36. Bosteels C, Neyt K, Vanheerswynghels M, van Helden MJ, Sichien D, Debeuf N, De Prijck S, Bosteels V, Vandamme N, Martens L, Saeys Y, Louagie E, Lesage M, Williams DL, Tang SC, Mayer JU, Ronchese F, Scott CL, Hammad H, Guilliams M, Lambrecht BN. Inflammat
37. Fasnacht N, Huang HY, Koch U, Favre S, Auderset F, Chai Q, Onder L, Kallert S, Pinschewer DD, MacDonald HR, Tacchini-Cottier F, Ludewig B, Luther SA, Radtke F. Specific fibroblastic niches in secondary lymphoid organs orchestrate distinct Notch-regulated

675 38. Briseño CG, Satpathy AT, Davidson JT 4th, Ferris ST, Durai V, Bagadia P, O'Connor KW,
676 Theisen DJ, Murphy TL, Murphy KM. Notch2-dependent DC2s mediate splenic germinal
677 center responses. Proc Natl Acad Sci U S A. 2018 Oct 16;115(42):10726-10731.
678 39. Kirkling ME, Cytlak U, Lau CM, Lewis KL, Resteu A, Khodadadi-Jamayran A, Siebel CW, Salmon
679 H, Merad M, Tsirigos A, Collin M, Bigley V, Reizis B. Notch Signaling Facilitates In Vitro
680 Generation of Cross-Presenting Classical Dendritic Cells. Cell Rep. 2018
681 40. Fujita K, Chakarov S, Kobayashi T, Sakamoto K, Voisin B, Duan K, Nakagawa T, Horiuchi K,
682 Amagai M, Ginhoux F, Nagao K. Cell-autonomous FLT3L shedding via ADAM10 mediates
683 conventional dendritic cell development in mouse spleen. Proc Natl Acad Sci U S A. 2
684 41. Van Gassen S, Callebaut B, Van Helden MJ, Lambrecht BN, Demeester P, Dhaene T, Saeys Y.
685 FlowSOM: Using self-organizing maps for visualization and interpretation of cytometry data.
686 Cytometry A. 2015 Jul;87(7):636-45.
687 42. Kasper M, Heming M, Schafflick D, Li X, Lautwein T, Meyer zu Horste M, Bauer D, Walscheid
688 K, Wiendl H, Loser K, Heiligenhaus A, Meyer zu Horste G. Intra-ocular dendritic cells are
689 increased in HLA-B27 associated acute anterior uveitis. bioRxiv 2021.02.16
690 43. Heger L, Balk S, Lühr JJ, Heidkamp GF, Lehmann CHK, Hatscher L, Purbojo A, Hartmann A,
691 Garcia-Martin F, Nishimura SI, Cesnjevar R, Nimmerjahn F, Dudziak D. CLEC10A Is a Specific
692 Marker for Human CD1c+ Dendritic Cells and Enhances Their Toll-Like Receptor
693 44. Jimenez-Dalmaroni MJ, Xiao N, Corper AL, Verdino P, Ainge GD, Larsen DS, Painter GF, Rudd
694 PM, Dwek RA, Hoebe K, Beutler B, Wilson IA. Soluble CD36 ectodomain binds negatively
695 charged diacylglycerol ligands and acts as a co-receptor for TLR2. PLoS One. 20
696 45. Obermoser G, Pascual V. The interferon-alpha signature of systemic lupus erythematosus.
697 Lupus. 2010 Aug;19(9):1012-9.
698 46. Horai R, Zárate-Bladés CR, Dillenburg-Pilla P, Chen J, Kielczewski JL, Silver PB, Jittayasothorn
699 Y, Chan CC, Yamane H, Honda K, Caspi RR. Microbiota-Dependent Activation of an
700 Autoreactive T Cell Receptor Provokes Autoimmunity in an Immunologically Privi
701 47. Horai R, Caspi RR. Microbiome and Autoimmune Uveitis. Front Immunol. 2019 Feb
702 19;10:232.
703 48. Ko HJ, Hong SW, Verma R, Jung J, Lee M, Kim N, Kim D, Surh CD, Kim KS, Rudra D, Im SH.
704 Dietary Glucose Consumption Promotes RALDH Activity in Small Intestinal CD103+CD11b+
705 Dendritic Cells. Front Immunol. 2020 Aug 11;11:1897.
706 49. Croxford AL, Lanzinger M, Hartmann FJ, Schreiner B, Mair F, Pelczar P, Clausen BE, Jung S,
707 Greter M, Becher B. The Cytokine GM-CSF Drives the Inflammatory Signature of CCR2+
708 Monocytes and Licenses Autoimmunity. Immunity. 2015 Sep 15;43(3):502-14.
709 50. Bing SJ, Silver PB, Jittayasothorn Y, Mattapallil MJ, Chan CC, Horai R, Caspi RR. Autoimmunity
710 to neuroretina in the concurrent absence of IFN-γ and IL-17A is mediated by a GM-CSF-driven
711 eosinophilic inflammation. J Autoimmun. 2020 Nov;114:102507.
712 51. Jabs DA, Nussenblatt RB, Rosenbaum JT; Standardization of Uveitis Nomenclature (SUN)
713 Working Group. Standardization of uveitis nomenclature for reporting clinical data. Results of
714 the First International Workshop. Am J Ophthalmol. 2005 Sep;140(3):509-16.
715 52. Kirkling ME, Cytlak U, Lau CM, Lewis KL, Resteu A, Khodadadi-Jamayran A, Siebel CW, Salmon
716 H, Merad M, Tsirigos A, Collin M, Bigley V, Reizis B. Notch Signaling Facilitates In Vitro
717 Generation of Cross-Presenting Classical Dendritic Cells. Cell Rep. 2018
718 53. Laban KG, Rijken R, Hiddingh S, Mertens JS, van der Veen RLP, Eenhorst CAE, Pandit A,
719 Radstake TRDJ, de Boer JH, Kalmann R, Kuiper JJW. cDC2 and plasmacytoid dendritic cells
720 diminish from tissues of patients with non-Hodgkin orbital lymphoma and idiopath
721 54. Ellis B, Haaland P, Hahne F, Le Meur N, Gopalakrishnan N, Spidlen J, Jiang M, Finak G (2020).
722 flowCore: flowCore: Basic structures for flow cytometry data. R package version 2.2.0.
723 55. Wilkerson, D. M, Hayes, Neil D (2010). "ConsensusClusterPlus: a class discovery tool with
724 confidence assessments and item tracking." Bioinformatics, 26(12), 1572-1573.
725 56. Wu H, Wang C, Wu Z. PROPER: comprehensive power evaluation for differential expression
726 using RNA-seq. Bioinformatics. 2015 Jan 15;31(2):233-41.

57. Cheung VG, Nayak RR, Wang IX, Elwyn S, Cousins SM, Morley M, Spielman RS. Polymorphic cis- and trans-regulation of human gene expression. PLoS Biol. 2010 Sep 14;8(9):e1000480.
58. Dobin A, Davis CA, Schlesinger F, Drenkow J, Zaleski C, Jha S, Batut P, Chaisson M, Gingeras TR. STAR: ultrafast universal RNA-seq aligner. Bioinformatics. 2013 Jan 1;29(1):15-21.
59. Anders S, Pyl PT, Huber W. HTSeq--a Python framework to work with high-throughput sequencing data. Bioinformatics. 2015 Jan 15;31(2):166-9.
60. Love MI, Huber W, Anders S. Moderated estimation of fold change and dispersion for RNA-seq data with DESeq2. Genome Biol. 2014;15(12):550.
61. Langfelder P, Horvath S. WGCNA: an R package for weighted correlation network analysis. BMC Bioinformatics. 2008 Dec 29;9:559.
62. Chen J, Bardes EE, Aronow BJ, Jegga AG. ToppGene Suite for gene list enrichment analysis and candidate gene prioritization. Nucleic Acids Res. 2009 Jul;37(Web Server issue):W305-11.
63. Davis S, Meltzer PS. GEOquery: a bridge between the Gene Expression Omnibus (GEO) and BioConductor. Bioinformatics. 2007 Jul 15;23(14):1846-7.
64. Ritchie ME, Phipson B, Wu D, Hu Y, Law CW, Shi W, Smyth GK. limma powers differential expression analyses for RNA-sequencing and microarray studies. Nucleic Acids Res. 2015 Apr 20;43(7):e47.
65. Jung D, Ge X (2020). PPInfer: Inferring functionally related proteins using protein interaction networks. R package version 1.16.0.

Funding: The presented work is supported by UitZicht (project number 2014-1). The funders had no role in the design, execution, interpretation, or writing of the study.

Author contributions:

Conceptualization: JK,TR,JB

Methodology: JK,SH,AP,FV,RR,NS,CW

Investigation: SH,AP,FV,RR,NS,CW,ND,SI

Visualization: JK,AP,RR

Funding acquisition: JK,JB,TR,SI

Project administration: JK,JB,FH,ND

Supervision: JK,TR,JB

Writing – original draft: SH,AP,FH,JK

Writing – review & editing: All authors

Competing interests: Authors declare that they have no competing interests

Figures:

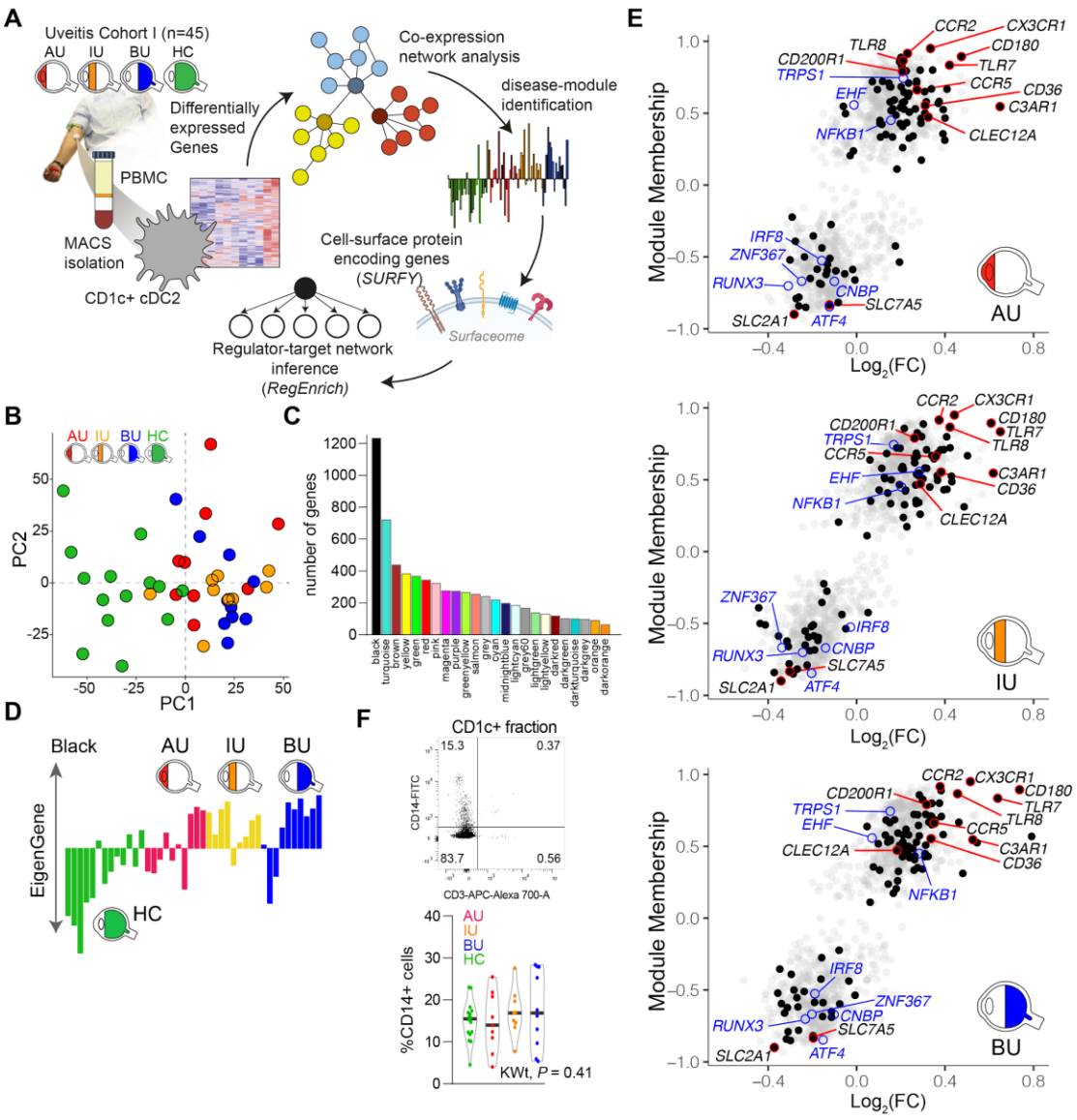

Fig. 1. A CD1c+ Dendritic cell (CD1c+ DC) transcriptional network is increased in expression in human autoimmune uveitis. A) Study design. CD1c+ DCs were purified from blood and subjected to RNA sequencing. Co-expression network analysis of differentially expressed genes was used to identify gene modules associated with uveitis and focus on the surface-protein encoding genes (predicted by *SURFY*[28]) and their transcriptional regulators (predicted by *RegEnrich*[32]). **B**) Principal component analysis of the 6,795 differentially expressed genes. **C**) Number of genes for each of the 24 identified gene modules. **D**) The *eigengene* values for the black module (y-axis) for each sample of cohort 1 (x-axis). **E**) The module membership (y-axis) and the (Log2) fold change in gene expression compared to healthy controls (x-axis) for genes in the black module in patients with AU (top), IU (middle), and BU (bottom). The 100 genes encoding surface proteins are indicated in black. Key transcription factors associated with functionally distinct CD1c+ DC subsets[29] are indicated in blue. **F**) The percentage of CD14-positive cells in the CD19(-) CD303(-) CD1c(+) cell fractions used for RNA sequencing. KWt; Kruskal-wallis test. AU; Anterior uveitis. IU; Intermediate uveitis. BU; Birdshot uveitis.

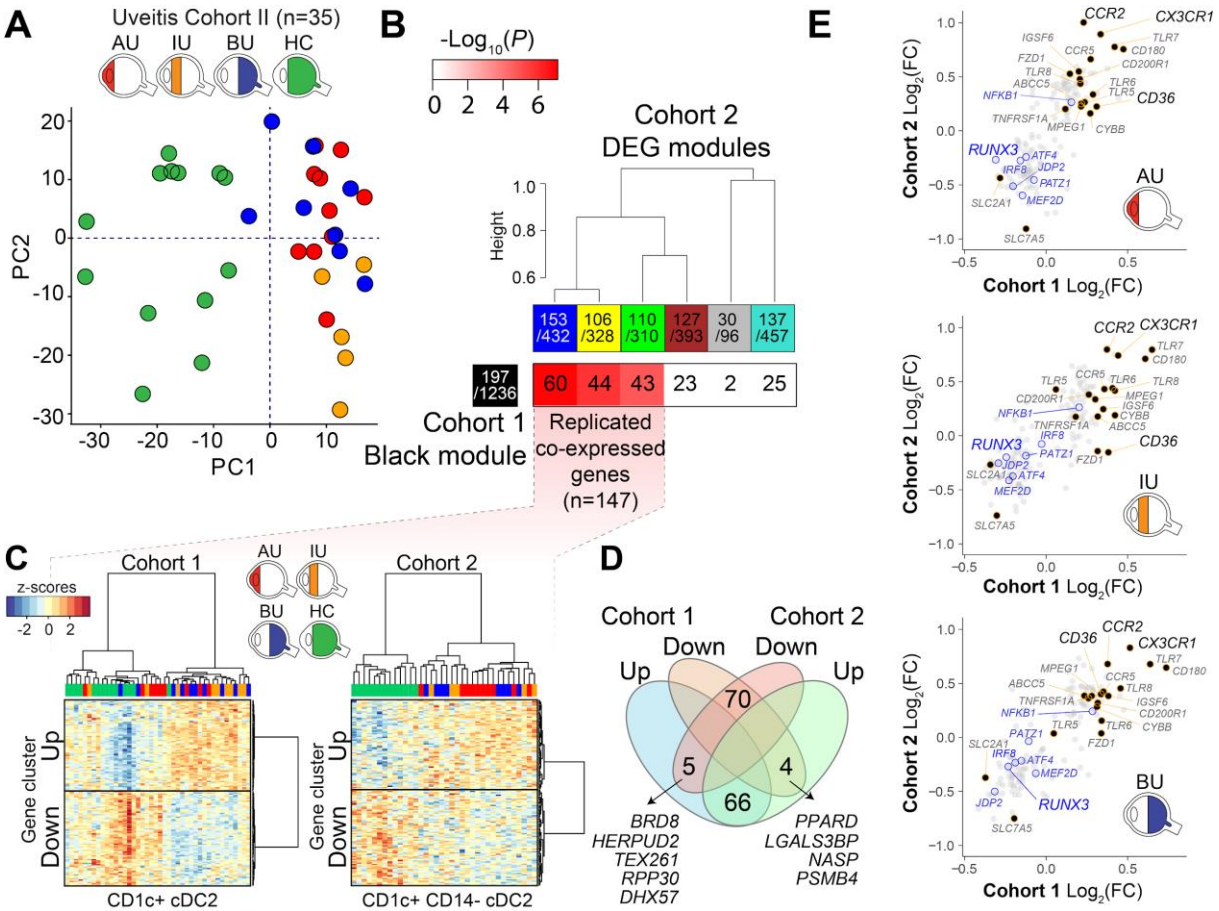

Fig. 2. Independent replication of the CD1c+ Dendritic cell (DC) core transcriptional signature in autoimmune uveitis. A) Principal component analysis of the 2,016 DEGs (*P*<0.05) in 35 patients and control samples of cohort 2. **B**) Cross-tabulation of the preservation of co-expressed genes from the black module in the second cohort. Each row and each column are labeled by the corresponding module color and the total number of genes in the module. The numbers represent the counts of genes in the intersection of the black module and modules identified in the second cohort. *P* value is from Fisher's exact test. Note that 147 co-expressed genes of the black module from cohort 1 are preserved across the blue, yellow and green modules of cohort 2, indicating co-expression for these genes across the two cohorts. **C**) Heatmaps of the 147 replicated co-expressed genes (rows) for samples (columns) from cohort 1 and cohort 2. **D**) Venn diagram of the upregulated and downregulated genes (clusters shown in **Fig. 2C**) from cohort 1 and 2. **E**) The (Log2) fold change in gene expression compared to healthy controls (x-axis) for all 147 replicated genes in patients with AU, IU, AND BU. Genes encoding surface proteins are indicated in black/grey. Key transcription factors associated with the surface-encoding genes identified by *RegEnrich*[32] are indicated in blue. AU; Anterior uveitis. IU; Intermediate uveitis. BU; Birdshot uveitis.

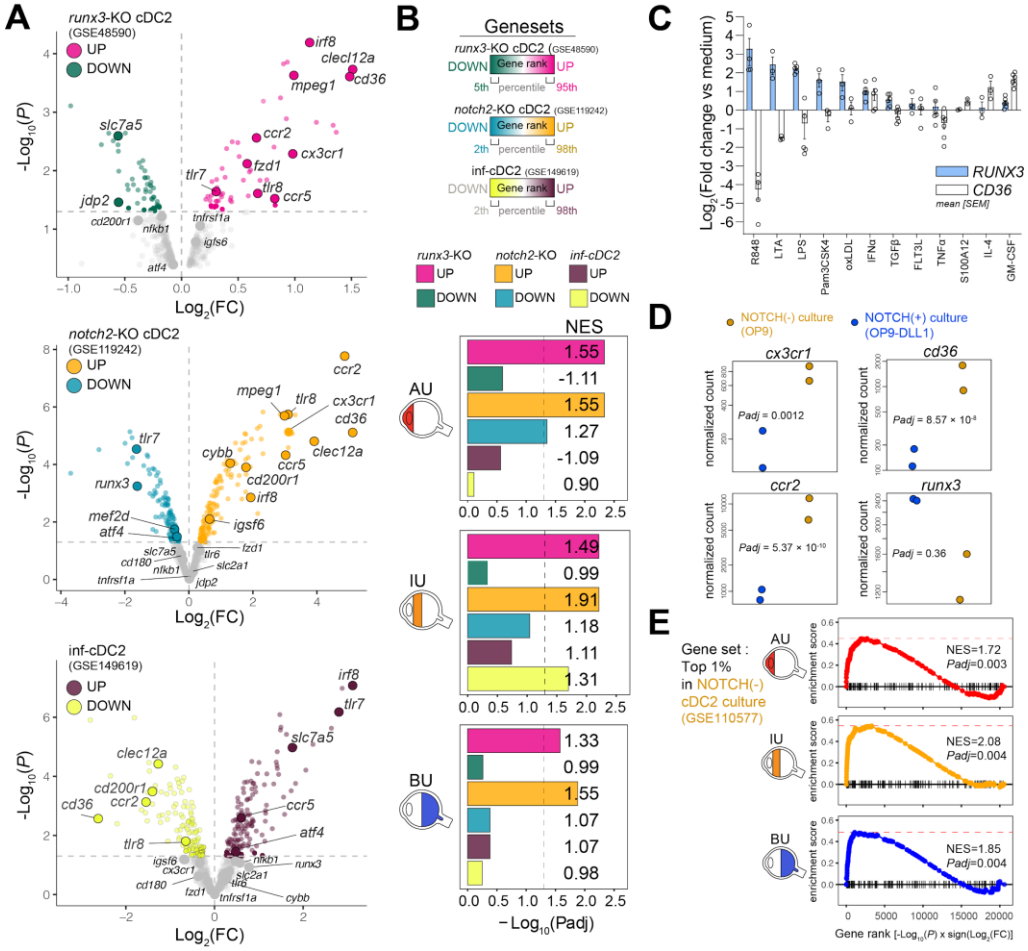

Fig. 3. Loss of NOTCH2-RUNX3 signaling in CD1c+ Dendritic cells (CD1c+ DCs) recapitulates the transcriptional signature of autoimmune uveitis. A) Volcano plot for the expression of genes of the black module in cDC2s of *runx3*-KO mice (GSE48590), *notch2*-KO mice (GSE119242), and inflammatory [inf-]cDC2s (GSE149619). Red dots denote the up-regulated genes and blue dots denote the down-regulated genes in cDC2s of each condition; grey dots denote the genes with no significant change in expression. Key genes identified in the uveitis cohorts (see **Fig. 2E**) are labeled. **B**) Results from gene-set enrichment analysis for 20,668 ranked genes (with baseMean>4) for AU, IU, and BU patients. The top or bottom percentiles of the ranked [$-\log_{10}(P)\times$ sign($\log_2$(FC))] genes from *runx3*-KO cDC2s, *notch2*-KO cDC2s, and inf-cDC2s (see *a*) were used as gene sets (all <500 genes). Normalized enrichment scores (NES) and *P* values (calculated by *Fast Gene Set Enrichment Analysis* R package, see methods) for each gene set is indicated. The dotted lines indicate *Padj* = 0.05. **C**) Gene expression (mean[SEM]) for *RUNX3* and *CD36* in primary human CD1c+ DCs from healthy donors stimulated overnight with Toll-like receptor ligands and cytokines implicated in dendritic cell biology. Each dot represents a single donor used in the experiment. **D**) Normalized counts (and adjusted *P* values from *DESeq2*) for *cx3cr1*, *ccr2*, *cd36*, and *runx3* from cDC2s (GSE110577) generated from murine bone marrow cells and OP-9 with (in blue) or without (in ochre) Notch ligand Delta-like 1 (DLL1). **E**) Gene set enrichment analysis similar to *b,* using the top 1%, (n=202) genes associated with the NOTCH-negative condition in *d* as the gene set. AU = Anterior uveitis. IU = Intermediate uveitis. BU = Birdshot uveitis. R848 = Resiquimod, LTA = Lipoteichoic acid, LPS = Lipopolysaccharides, Pam3CSK4 = Pam3CysSerLys4, OxLDL = Oxidized low-density lipoprotein, IFNα = Interferon alpha, TGFβ = transforming growth factor beta. FLT3L = FMS-like tyrosine kinase 3 ligand, TNFα = tumor necrosis factor alpha, S100A12 = S100 calcium-binding protein A12, IL-4 = interleukin 4, GM-CSF = Granulocyte-macrophage colony-stimulating factor.

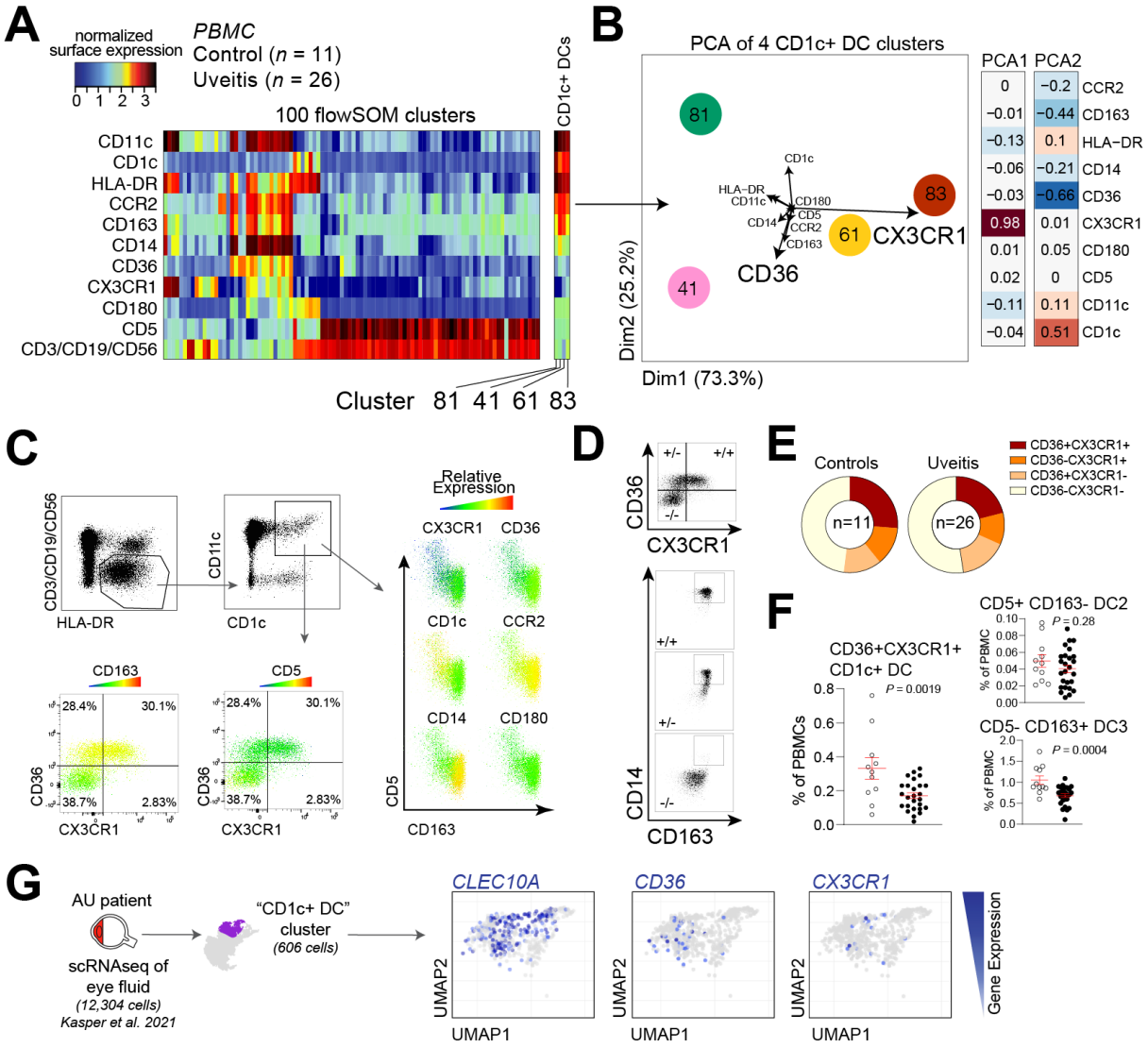

Fig. 4. A subset of CD36+CX3CR1+CD1c+ Dendritic cells (CD1c+ DCs) is decreased in circulation of patients with autoimmune uveitis. A) Heatmap of the surface protein expression for the 100 flowSOM clusters of 11-parameter flow-cytometry analysis of PBMC samples from 26 cases and 11 controls. The four CD1c+ (CD3-CD19-CD56-HLA-DR+CD11c+) DC clusters identified (cluster 41, 61, 81, and 83) are highlighted. **B**) PCA biplot of the surface protein expression for CD36, CX3CR1, CCR2, CD5, CD163, CD14, CD11c, HLA-DR, and CD180 in flowSOM clusters 41, 61, 81, and 83 identified in *a*. The loadings for PC1 and PC2 are shown on the right. **C**) Flow cytometric example of manual gating strategy of CD1c+ DC subsets showing the (color-coded) relative expression for CD5 and CD163 in a biplot of CD36 and CX3CR1. The color-coded relative expression for CD36, CX3CR1, CD1c, CCR2, CD14, and CD180 is shown in a biplot of CD5 and CD163 on the right (representative example of n = 37). **D**) Biplot of CD14 and CD163 in each of the identified CD1c+ DC subsets based on CD36 and CX3CR1. **E**) The relative proportion of CD1c+ DC subsets based on CD36 and CX3CR1 among total CD1c+ DCs and **F**) the frequency of CD36+CX3CR1+ CD1c+ DCs, and CD5+CD163- DC2s and CD5-CD163+ DC3 cells among PBMCs in uveitis cases and controls. *P* values from unpaired *t* test. **G**) UMAP projections of transcriptomic data from 606 CD1c+ DC cells from eye fluid from 4 (HLA-B27-positive) AU patients ("DC2" cluster from *Kasper et al. 2021* (*54*)). The eye-infiltrated CD1c+ DCs are shown in grey, cells expressing *CLEC10A (*CD1c+ DC tissue marker*), CD36,* or *CX3CR1* are indicated in blue. Plots were generated with https://osmzhlab.uni-muenster.de/shiny/cerebro_uveitis/. AU = Anterior uveitis.

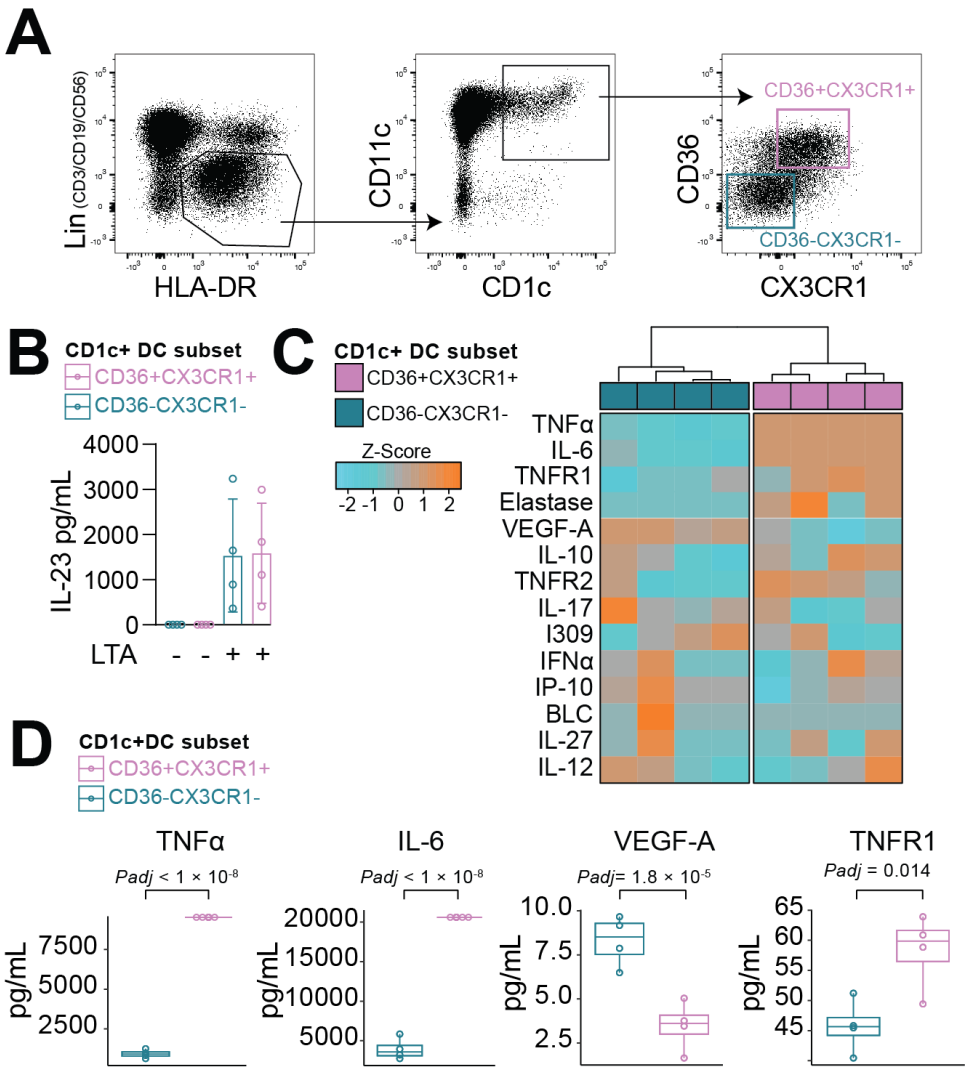

Fig. 5. CD36+CX3CR1+CD1c+ Dendritic cells (DCs) are functionally distinct A) The gating strategy to sort primary human CD1c+ DC subsets based on the expression of CX3CR1 and CD36 for downstream analysis. The CD1c+ DC cells were FACS sorted into CD36+CX3CR1+ and CD36-CX3CR1- CD1c+ DCs. **B**) The concentration of IL-23 (ELISA) in supernatants of 18h cultured primary human CD1c+ DC subsets cells stimulated with lipoteichoic acid (LTA). **C**) Heatmap of the levels (Z-score) of 16 detected proteins in supernatants of 18h cultured LTA-stimulated primary human CD1c+ DC subsets cells using an in-house multiplex *Luminex* assay. **D**) Scatter plots with overlay boxplot with mean and interquartile range of the levels of secreted TNF-alpha, Interleukin(IL)-6, VEGF-A, and TNFR1 from the multiplex protein data in *d.* (*Padj* = *P* values from likelihood ratio test Bonferroni corrected for 16 detected proteins)

Table 1.

Discovery cohort	AU	IU	BU	HC	*P* value
N	9	9	10	16	n.a.
Male / Female	3/6	2/7	4/6	6/10	0.90*
Age in years; mean ± SD	47.7 ± 17.0	39.3 ± 14.0	52.9 ± 13.2	41.4 ± 9.8	0.09**
Disease duration in years; median (range)	5.8 (0.1-39.3)	3.7 (0.2-20.0)	1.3 (0.2-15.1)	n.a.	0.14***
Replication cohort	**AU**	**IU**	**BU**	**HC**	***P* value**
N	10	5	8	13	
Male / Female	2/8	3/2	5/3	5/8	0.25*
Age in years; mean ± SD	45.9 ± 16.1	29.9 ± 10.7	42.1 ± 10.5	42.2 ± 13.3	0.20**
Disease duration in years; median (range)	8.1 (0.2-22.3)	3.4 (0.4-14.1)	0.9 (0.2-19.9)	n.a.	0.36***

Table 1. Characteristics of the patients and controls from cohort 1 and cohort 2. Abbreviations: BU: Birdshot uveitis, AU: HLA-B27 associated anterior uveitis, HC: healthy control, IU: idiopathic intermediate uveitis, n.a.: not applicable, * Fisher's exact test, ** ANOVA,*** Kruskal-Wallis.

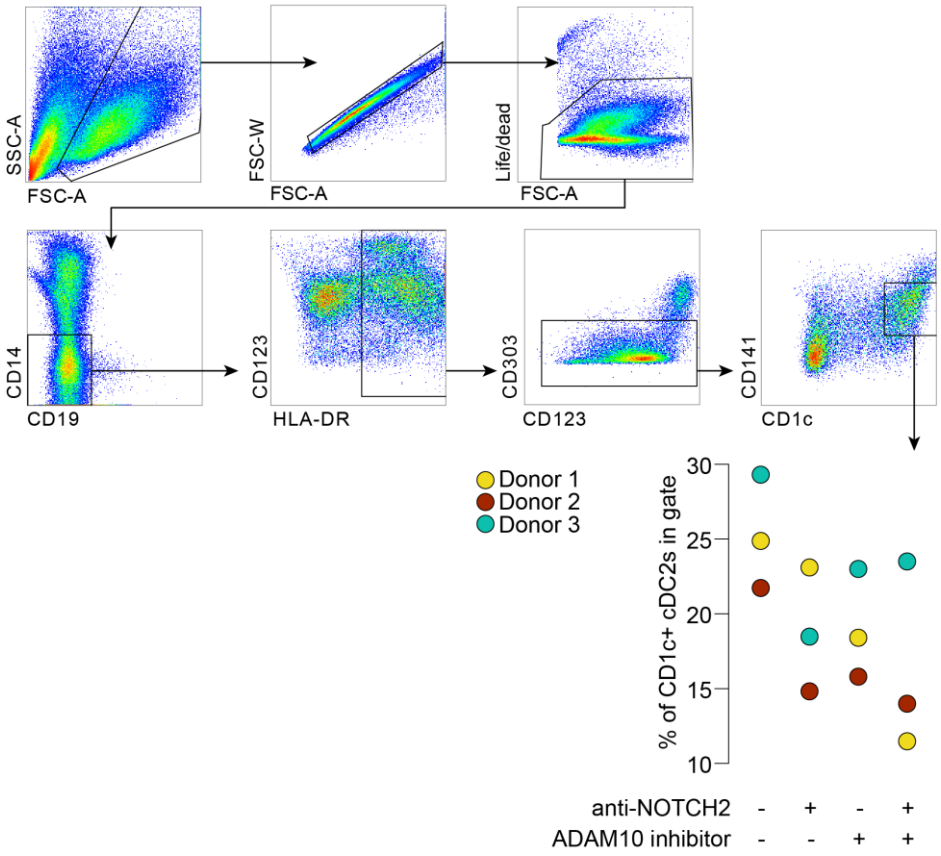

Supplemental Fig. S1. Flow cytometry analysis of CD1c+ DC cells generated from CD34+ hematopoietic cord blood after NOTCH2 and ADAM10 inhibition. CD34+ cells from umbilical cord blood mononuclear cells were cultured with OP-9 cells (see methods) After 7 days 10µM ADAM10 inhibitor (GI 254023X; R&D systems) or 50ng/mL anti-NOTCH2 (clone B6; Absolute Antibody) or a combination of the inhibitors were added to the cells and cultured for another 7 days. Cells were harvested and used for FACS analysis on day 14.

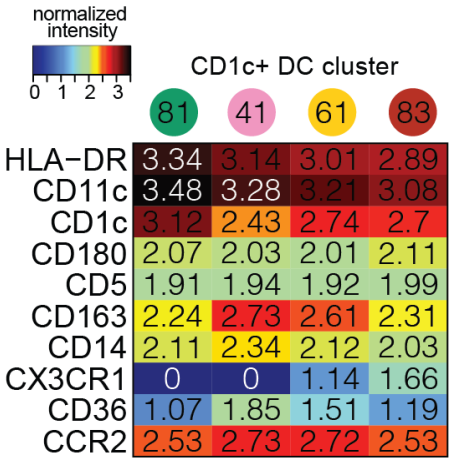

Supplemental Fig. S2. FlowSOM results for CD1c+ DC clusters in PBMCs. The normalized intensities of the protein expression of surface markers by the four CD1c+ DC clusters identified by flowSOM[41] in flow cytometry data from 11 controls and 26 autoimmune uveitis patients.

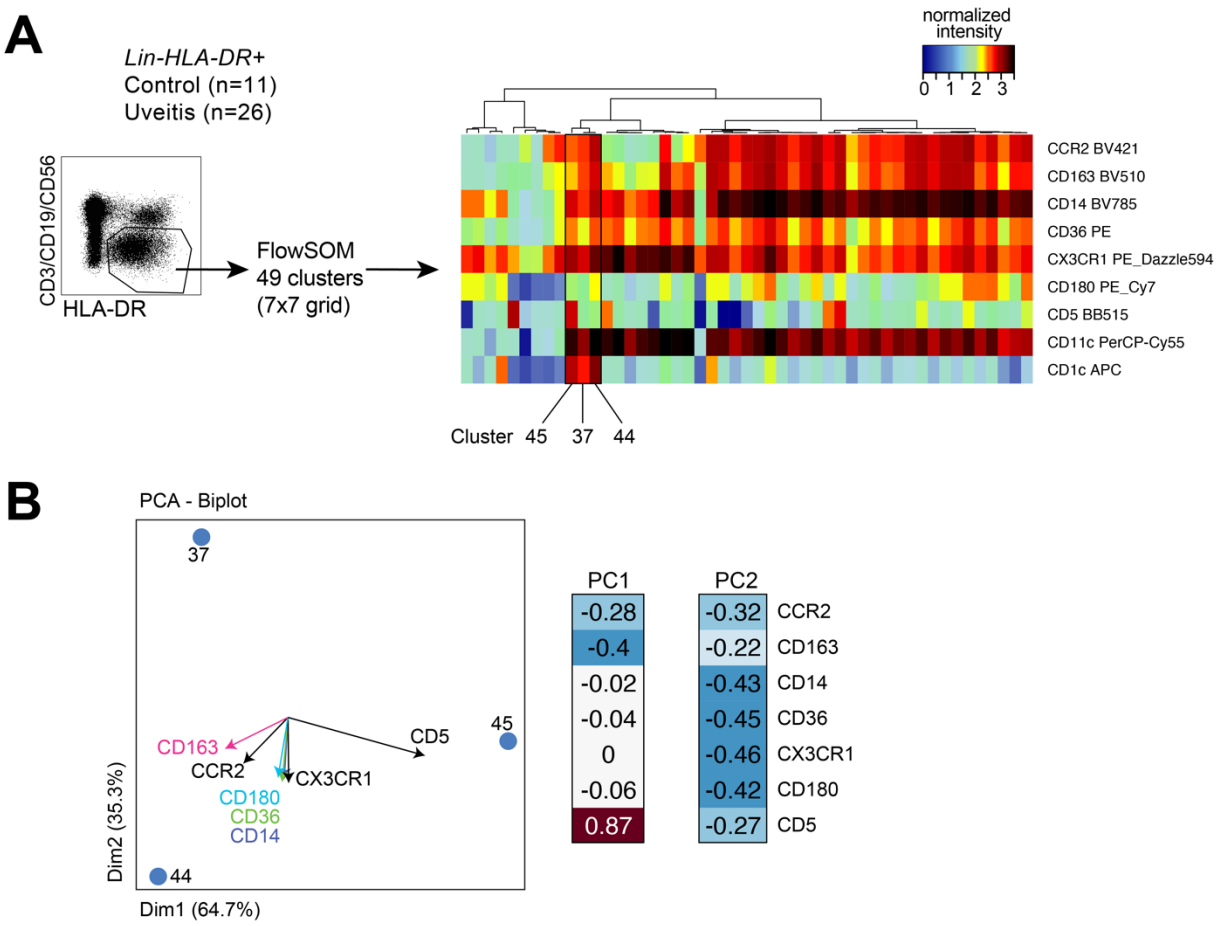

Supplemental Fig. S3. **FlowSOM analysis using Lineage (CD3/CD19/CD56) negative and HLA-DR-positive cells as input.** This analysis distinguished 3 CD1c+ DC phenotypes among a predetermined number of 49 clusters (7x7 grid). PCA biplot identified CD5 as a top loading in PC1 and CX3CR1 and CD36 as top loadings in PC2 among the three CD1c+ DC subsets in Lin-HLA-DR+ cells. These data support that genes associated with autoimmune uveitis (i.e., CX3CR1 and CD36) encode surface markers that distinguish CD1c+ DC phenotypes. **A)** Heatmap for surface protein expression for 49 cell clusters (7x7 grid) identified by flowSOM[41] using Lineage (CD3/CD19/CD56) negative and HLA-DR-positive cells as input from 37 PBMC samples from cases and controls from this study. The three CD1c+ DC clusters identified in this analysis (population 37, 44, and 45) are highlighted. **B**) PCA Biplot of the normalized intensity data from flowSOM for CD36, CX3CR1, CCR2, CD5, CD163, CD14, and CD180. The loadings for PC1 and PC2 are shown on the right.

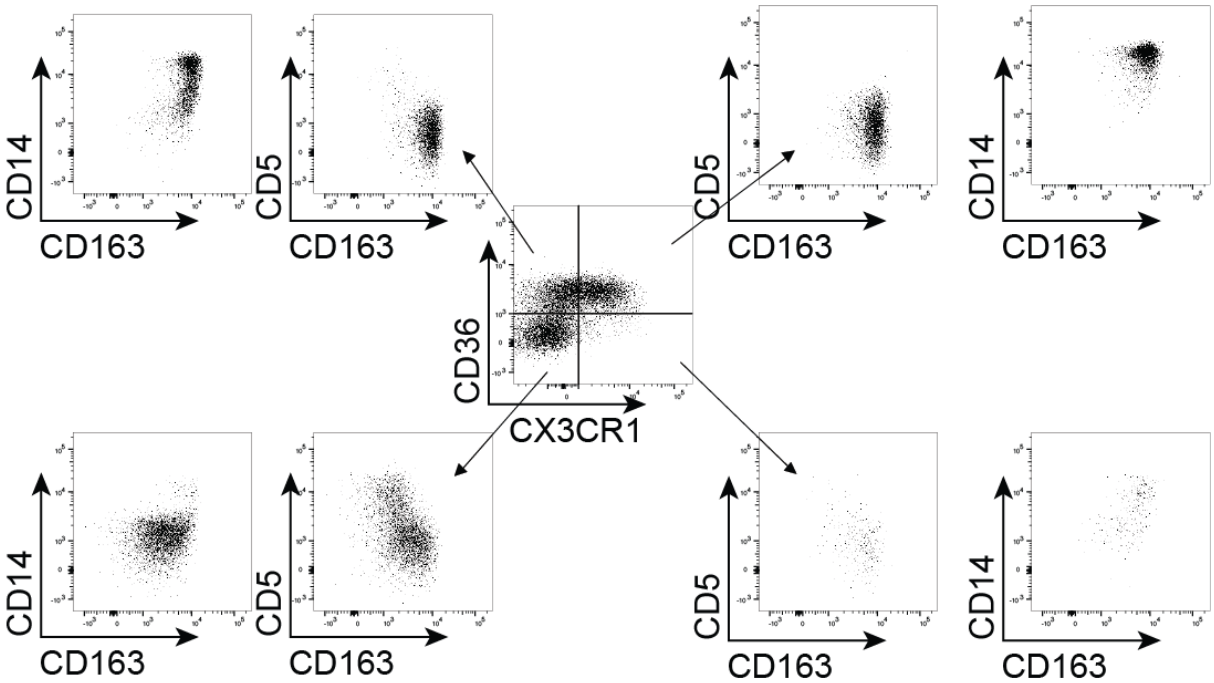

Supplemental Fig. S4. Flow cytometry gating example of CD1c+ CD11c+ DCs subsets based on CD36 and CX3CR1.